



GE HealthCare



White Paper

TrueFidelity DL for Spectral Imaging

**A new generation of spectral imaging powered by
deep learning**

Technical white paper on deep learning image reconstruction
for spectral imaging

Jean-Baptiste Thibault, Ph.D.; Brian Nett, Ph.D.; Jie Tang, Ph.D.;
Eugene Liu, M.D.

Contents

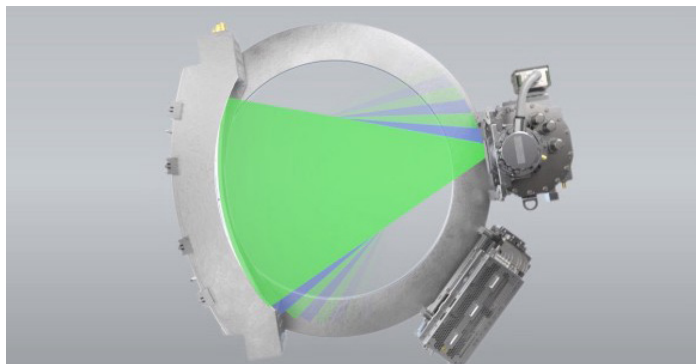
1. Introduction	3
2. The Next Generation of Spectral Powered by Deep Learning	5
3. Performance Evaluation	7
4. Clinical Examples	13
5. Conclusion	17
6. References	18

Introduction

Since 2010, dual-energy CT with Spectral Imaging¹ has demonstrated added diagnostic value across a wide range of clinical applications.²⁻⁸

Leveraging the unmatched speed of the scintillator at the heart of the CT detector, GSI realizes dual-energy acquisitions using a uniquely fast kV switching technology at double the angular sampling rate of single-energy acquisitions. This produces near-perfect spatial and temporal registration of the low/high energy measurements and supports spectral information for the full field-of-view of 50 cm.

The high-voltage generator that powers the X-ray tube has been designed to produce controlled kV transitions with an average of 60 microseconds across all scan techniques in order to preserve energy separation between the low and high kV spectra. More recently the Quantix X-ray tube was introduced on the Revolution Apex which features novel digital cathode technology that supports near-instantaneous adjustments in tube current⁹ and realizes synchronized kV and mA switching to balance the signal between low and high kV measurements.



Ultrafast kV switching technology

Contrary to some dual-energy techniques, GSI's all X-ray photons are effectively used to produce an accurate image of the patient without loss of dose efficiency. To make the best use of the spectral information in the measurements, GSI allows direct projection-based material decomposition for inherent reduction of beam hardening artifacts and higher quantitative accuracy than image domain techniques. In an independent comparison of competing dual-energy technologies, GSI on the Revolution CT platform was ranked the highest for iodine accuracy across a range of clinically relevant concentrations.¹⁰

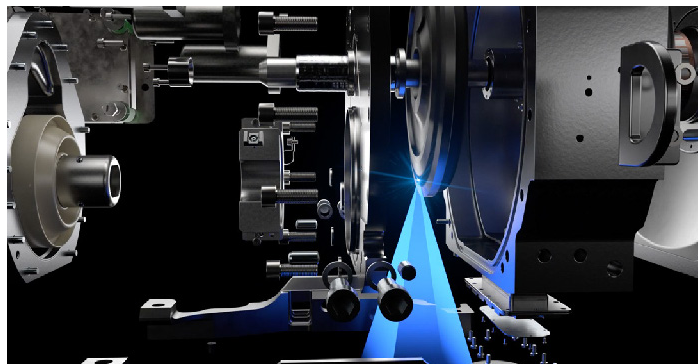
Spectral Imaging Highlights

With near-perfect spatial and temporal registration of the collected energy samples, fast kV switching supports quantitatively accurate spectral imaging in the full 50 cm field of view.

Through innovative projection domain material decomposition processing, GSI has shown benefits in:

- Providing details of chemical composition and material characteristics for better lesion characterization
- Improving lesion detection with enhanced contrast-to-noise ratio
- Reducing beam hardening and metal artifacts
- Optimizing iodine load in contrast enhanced CT studies

The Quantix tube features novel digital cathode technology that realizes synchronized kV and mA switching to positively impact iodine MD images and reduce noise on low keV images for small lesion detection and assessment.



Quantix tube with synchronized kV and mA switching

In addition to quantitative accuracy, the flexible clinical workflow of GSI enables effortless generation of the right images for different clinical scenarios directly from the scanner. The scanner can reconstruct monochromatic keV images in the range of [40-140] keV to tailor for either enhanced contrast or reduced beam hardening. Additional images sets that can be generated on the console include but are not limited to: water/iodine, material basis pairs like calcium and uric acid (HAP) for tissue characterization, and virtual unenhanced (VUE) images. A metal artifact-reduced (MAR) algorithm dedicated for GSI can also be applied to any of these image types. Once reconstructed, images can be automatically transferred to the PACS or a dedicated review station for the diagnostic read or further advanced processing.

These GSI image types have been used to address a multitude of clinical scenarios. keV images from projection-based material decomposition provide inherent beam hardening reduction and higher contrast than single energy images and can, for example, assist in subtle lesion detection in oncology.^{2,11,12} Likewise, iodine images can help better visualize bleeds and other lesions and blockages such as pulmonary embolisms.^{13,14} Other material images support quantitative tissue characterization, for instance, to assess the makeup of kidney stones, measure liver fat content, and identify post-traumatic bruising in bone tissue. The benefits of GSI extend all the way to potentially saving patient radiation dose when VUE is used to replace images from a non-contrast scan prior to the contrast-enhanced acquisition.¹⁵

As in all of CT acquisitions, when optimizing patient dose for least exposure, image noise remains a limiting factor for a quick and confident diagnosis. One of the characteristics of the material decomposition process is that image noise resulting from noisy low/high kV measurements is increased and becomes correlated (or related) between the different material basis selections (e.g. water and iodine chosen as the default basis pair). GSI fast kV switching partially compensates for this with longer time spent at 80 kV than 140 kV to increase statistics in the low-energy measurements. With synchronized kV/mA switching, the Revolution Apex platform also increases instantaneous flux in the 80 kV part of the acquisition. This improves low keV and iodine images that are most influenced by the low-energy measurements. In addition, GSI reconstruction was designed to have monotonic noise behavior as a function of keV to avoid an artificial peak of CNR at higher keV's than the lowest available energy. However, noise magnification in lower keV images is inherent in spectral imaging and typically more noticeable at or below 50 keV. Even with advanced processing and iterative reconstruction techniques built into the dual-energy image reconstruction flow, image noise may limit the contrast-to-noise ratio (CNR) of monochromatic images.

GE recently achieved a significant breakthrough for noise reduction by introducing TrueFidelity DL to improve image quality for single-energy acquisitions, with great success across many clinical applications.¹⁶⁻¹⁹ TrueFidelity DL is the first Deep Learning Image Reconstruction (DLIR) technique to have addressed the challenges of both conventional and iterative reconstruction.²⁰ By training on high-dose ground truth filtered back projection (FBP) images with desirable characteristics in terms of noise level and texture, TrueFidelity DL produces low-noise images that preserve a natural image texture and avoid the artificial, flat, and “plastic” look of iterative reconstruction methods applied to low-dose data.^{21,22} As a result, clinicians have been able to quickly adopt TrueFidelity DL across their entire CT practice and further optimize their protocols for adjusted patient dose. Building upon this experience, TrueFidelity DL is well-suited to further reduce noise and improve image texture in dual-energy images, and GE is pleased to introduce TrueFidelity DL for spectral applications.

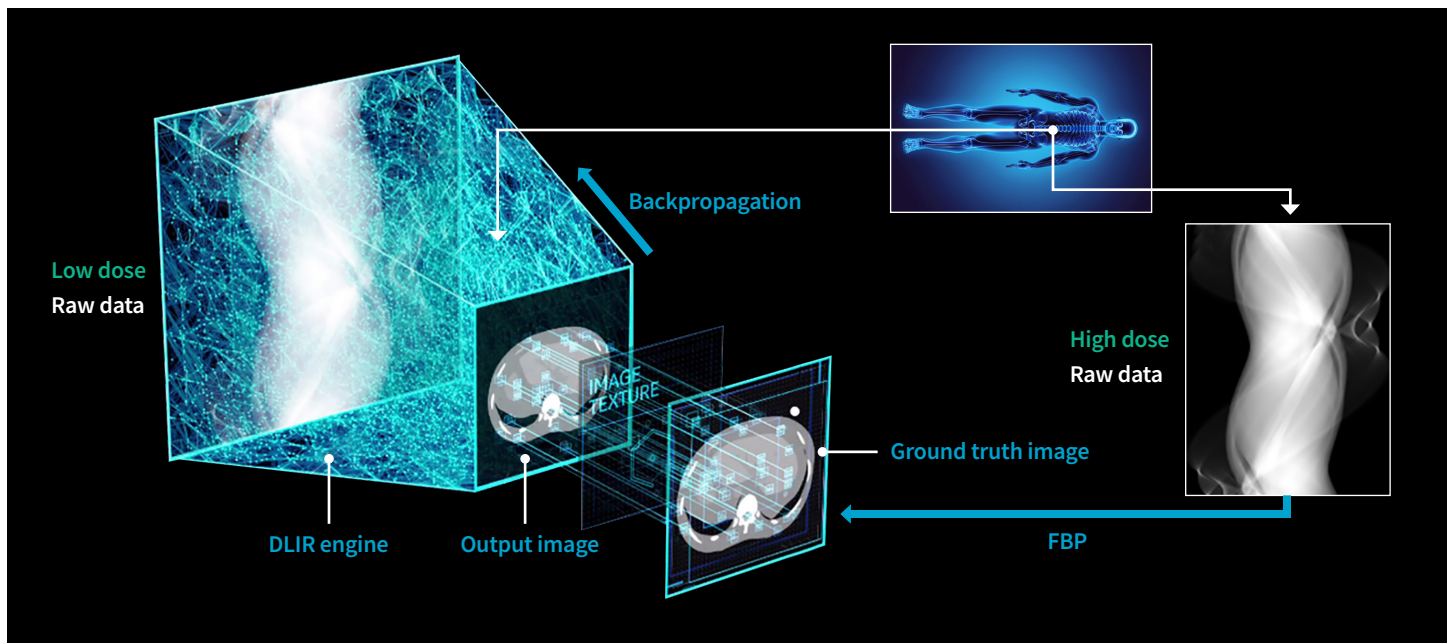


Figure 1: A schematic of the DLIR training process in single-energy application.

The Next Generation of Spectral Imaging Powered by Deep Learning

TrueFidelity DL was designed to produce image quality performance not easily achievable by conventional analytical and iterative techniques. Rather than manually optimizing the reconstruction over many parameters to balance image noise, spatial resolution, overall texture, and other quality metrics across a multitude of clinical imaging scenarios, the deep-learning approach uses a neural network to learn the desired characteristics of the reconstructed images. This produces a reconstruction model that is far more effective to represent the complex interactions between CT measurements and image data. With DLIR technology, GE was able to break through the image quality limitations lingering after years of manually optimizing iterative reconstruction methods that could still produce images that are too flat or artificial in appearance. These improvements were made possible by designing the training process to systematically learn the characteristics of high-quality images such that they could be reproduced when reconstructing data from more challenging low-dose and highly noisy measurements.

For single-energy scenarios, high-quality images from standard filtered back projection (FBP) reconstruction of high-dose high quality measurements were selected as the ground truth. Using high-quality FBP images rather than denoised reference images such as those obtained by hybrid or model-based iterative reconstruction allows TrueFidelity DL to preserve a natural image texture even after reducing image noise in challenging low-dose cases. The model is represented by a convolutional neural network (CNN) with multiple layers and thousands of inter-layer connections. The coefficients attached to each connection are trained to best recover ground truth images from noisier measurements. Once the coefficients of the model are learned via this offline process, the parameters are fixed, and images are reconstructed by processing new sinogram measurements with the CNN as designed. Once training is complete, reconstruction is very fast, allowing TrueFidelity DL to meet the most demanding clinical settings.

TrueFidelity DL for Spectral imaging Highlights

A new generation of spectral imaging powered by deep learning. Another industry first, with a bold vision to transform image quality for dual-energy spectral CT with TrueFidelity DL for Spectral images: Outstanding detail, clarity, texture, and dose, without compromise, for all GSI image types.

GE has now adapted this approach to GSI by appropriately accounting for the unique characteristics of dual-energy data. With the advantages of the GSI data acquisition approach outlined above, the benefits attached to performing material decomposition in the projection domain (high quantitative accuracy and inherent beam hardening reduction) are preserved. The TrueFidelity DL for Spectral image chain first produces material decomposed sinograms from the low/high kV measurements. Then the DLIR engine is tasked with learning the unique characteristics of the noise in both material bases (i.e. iodine and water) to reduce noise while preserving details and overall texture. Because spectral image types reconstructed with GSI, such as monochromatic (keV) images and other material basis pairs, are formed from a linear recombination of material basis images, it is necessary to process the data consistently for the native material basis pair of water/iodine.

TrueFidelity DL for Spectral imaging therefore learns the characteristics of the data in the material basis space, and jointly trains the parameters of the reconstruction model for both material basis components. Joint training guarantees that the reconstruction treats noise reduction and texture preservation similarly for each basis image component in order to avoid over-emphasis of any single component that could lead to artifacts in images transformed from the native material basis pair of water/iodine. Thus, a unified network across the materials (iodine/water) provides for consistency in the training and application of TrueFidelity DL for spectral imaging. This approach inherently enables TrueFidelity DL to extend its benefits to all GSI image types. Monochromatic (keV) images, other material decomposed basis pairs, VUE images, and MAR images all benefit similarly from TrueFidelity DL for Spectral imaging.

Like for single-energy, TrueFidelity DL for Spectral imaging is trained on high-quality high-dose FBP images of dual-energy acquisitions used as ground truth data. TrueFidelity DL for Spectral imaging can therefore emulate high-quality high-dose results even from lower-dose measurements. A robust training data set is created from both phantom and clinical data across multiple anatomies and contrast imaging conditions as well as many different noise realizations for various clinical imaging scenarios. The training process follows the same approach as for single-energy and focuses on producing similar results in terms of reducing noise magnitude as well as preserving overall image texture from any artificial degradation that could be due to advanced processing. TrueFidelity DL for Spectral imaging offers the same low/medium/high strength settings as TrueFidelity DL for single-energy data with similar denoising performance.

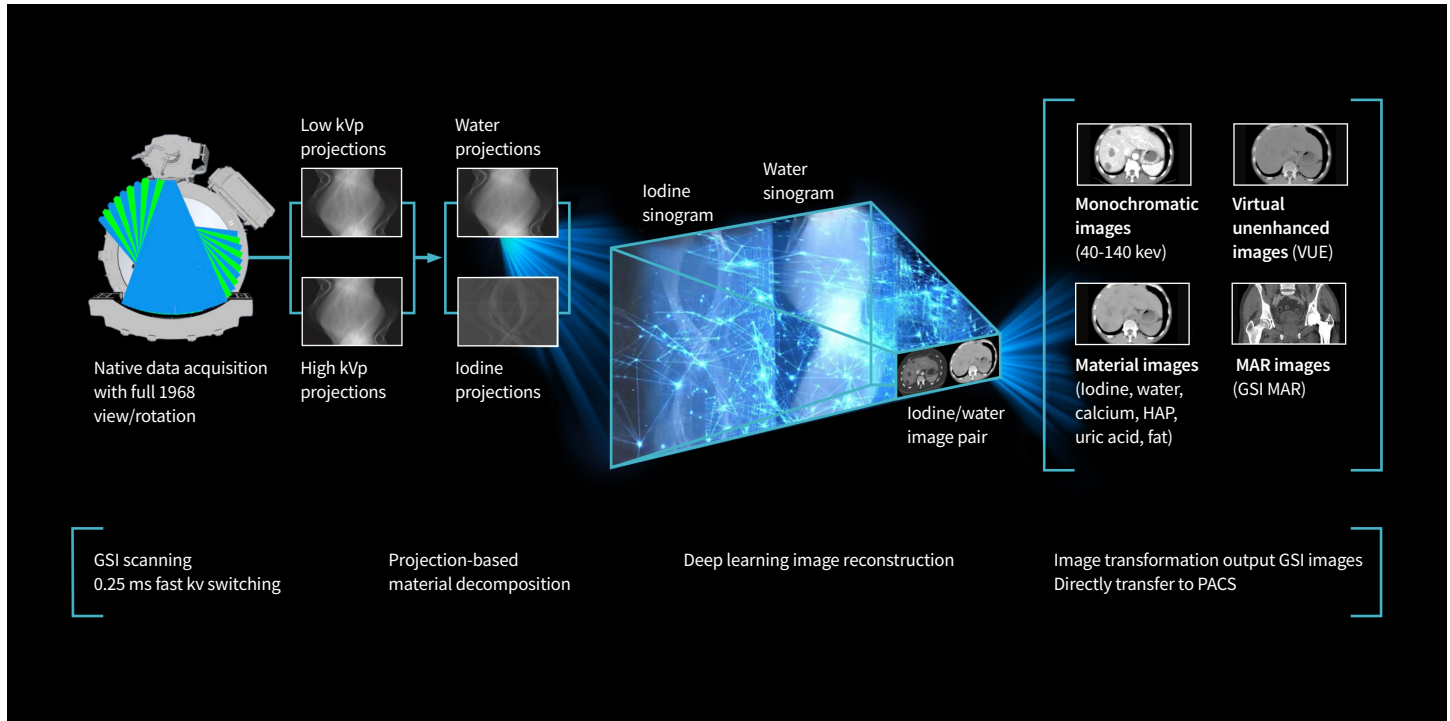


Figure 2: GE leverages deep learning reconstruction engine to generate GSI images.

TrueFidelity DL for Spectral imaging processes both material sinograms simultaneously to reconstruct images, representing about twice as much data as corresponding single-energy scans. In an effort to continuously improve on the overall workflow of the scanner, GE optimized the DLIR neural network using well-known model compression techniques to reduce computational load while preserving image quality performance even as the volume of data increases with GSI. The result is routinely fast reconstruction speed for daily processing needs, even for spectral imaging. For instance, TrueFidelity DL for Spectral imaging can reconstruct 585 0.625 mm images of a typical chest PE scan in less than 2 minutes on the Revolution CT and Revolution Apex scanners with the standard Wide Cone Reconstruction Server.*

TrueFidelity DL for Spectral imaging is implemented directly on the scanner as it would be for single-energy data. All GSI image types are supported, including all slice thicknesses and reconstruction orientations via Direct Multi-Planar Reformat (DMPR). Prescribed images are natively reconstructed on the console for the selected strength and automatically networked to the desired destinations for diagnostic review or further advanced post-processing.

* Measured stopwatch timing from clicking the run button until the reconstruction job is finished for a 80 mm p1.531, 0.5 s/rot, 585 slices, 0.625 mm, DLIR-H and AR70 take 1:58.20 and 1:18.58 min/sec, respectively, averaged over 4 runs when the reconstruction engine is otherwise idle.

Performance Evaluation

TrueFidelity DL for Spectral imaging delivers superior image quality performance compared to other current reconstruction technologies, including iterative reconstruction. To demonstrate these benefits, several key evaluation metrics are summarized in this section, spanning both bench testing and clinical reader study results.

High noise (in terms of pixel standard deviation) may reduce the diagnostic value of clinical images. Like for single-energy, TrueFidelity DL for Spectral imaging was designed to reduce image noise compared to current iterative reconstruction technology, such as ASiR-V, at the same dose (CTDIvol). A rigorous comparison of image noise levels was done on the Revolution Apex using the uniform section of the Catphan® 600 phantom with the CTP579 oval body annulus** to simulate a typical adult body as shown in Figure 3. Both ASiR-V at 50% strength (AR50) and the high setting of TrueFidelity DL for Spectral imaging (DL-H) were reconstructed from three clinically representative CTDIvol dose levels at 5.84 mGy, 11.01 mGy, and 17.29 mGy, achieved by adjusting the mA for the GSI scans. Note that AR50 is the most frequently used level and recommended for clinical practice. Each scan was repeated five times over each dose level to increase sample size, and noise statistics from a 4x4 cm ROI in the uniform center section were averaged over 80 images per scan and 8 images per scan for 0.625 mm slice thickness. Figure 4 demonstrates that DL-H images have lower noise than AR50 images across all image types (40 keV, 70 keV, water (iodine) and iodine (water) images) regardless of dose. The same result extends to larger slice thicknesses by a similar scaling factor.

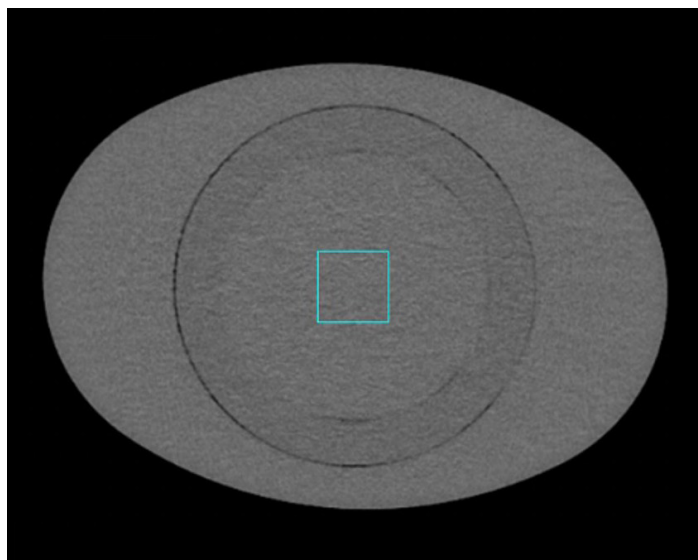


Figure 3: Uniformity section of the Catphan 600 with an added annulus to simulate the attenuation of a typical adult body, with a 4x4 cm centered ROI for noise measurements.

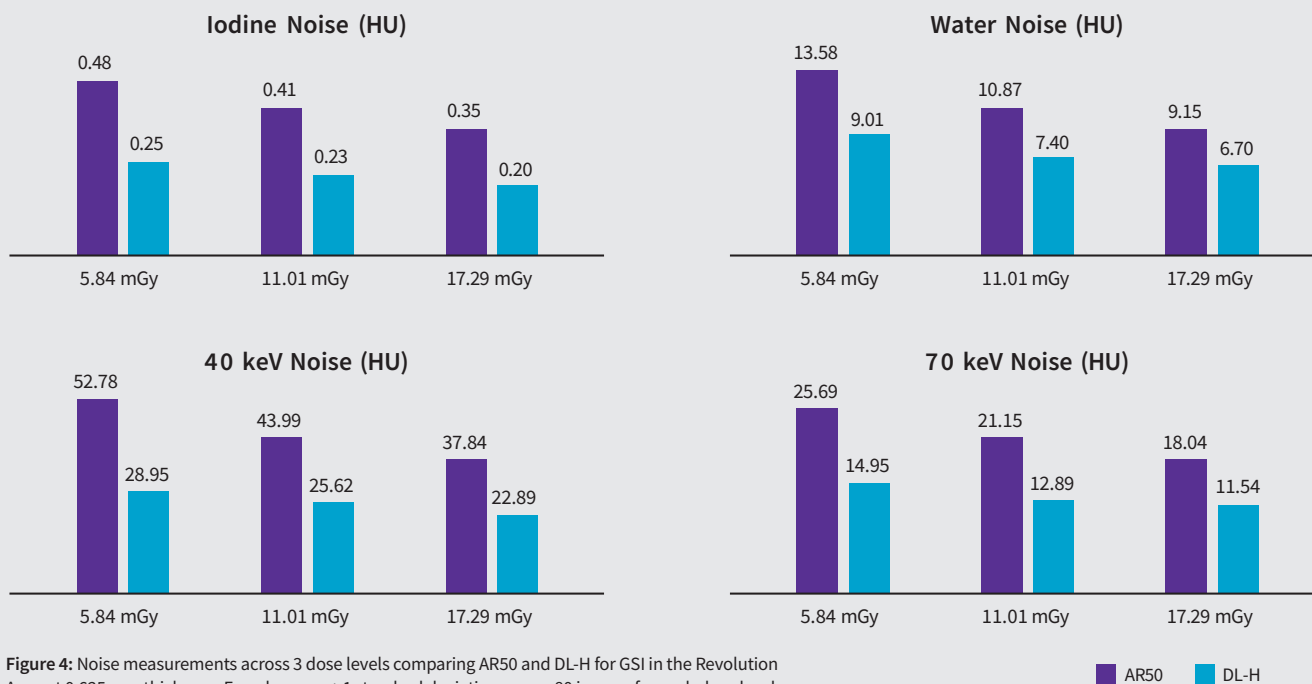


Figure 4: Noise measurements across 3 dose levels comparing AR50 and DL-H for GSI in the Revolution Apex at 0.625 mm thickness. Error bars are ± 1 standard deviation across 80 images for each dose level.

** Part numbers CTP486 and CTP579, respectively, from The Phantom Laboratory, Salem, NY.

While TrueFidelity DL for Spectral imaging is very effective at reducing image noise, it also succeeds at accomplishing this goal without compromising spatial resolution performance or artifacts. Figure 5 illustrates on the resolution bar section of the Catphan phantom that image texture, noise, and resolution performance are comparable between single and dual energy with fast kV switching when reconstructing with TrueFidelity DL. This shows the benefit of the fast kV switching approach with GSI that builds upon the extremely fast switching speed of the generator and fast response of the detector to conserve spatial sampling with twice the number of samples relative to single-energy combined with TrueFidelity DL reconstruction to manage image noise, texture and artifacts. Slower kV switching may result in lower resolution and increased aliasing streaks and artifacts if it cannot operate as fast as GSI, especially for anatomical features located further away from the isocenter. Figure 5 also illustrates that image quality performance is generally equivalent between TrueFidelity DL for single-energy and GSI dual-energy for both natural image texture and noise reduction magnitude.

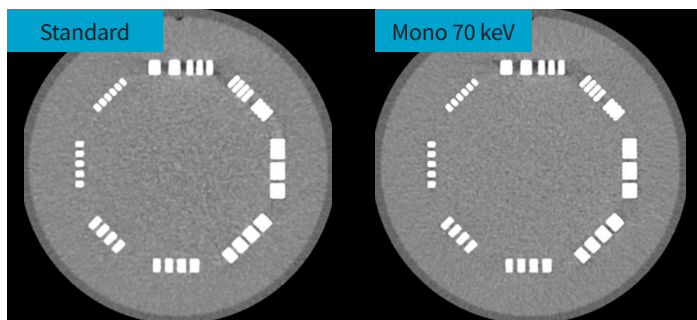


Figure 5: Comparison of TrueFidelity DL images for single-energy (left – 120 kV) and dual-energy (right – GSI, monochromatic 70 keV) on the section of the Catphan phantom with visual resolution bars. Images are with the Standard kernel with 0.625 mm slice thickness and the DL-H setting, illustrating similar visual resolution, noise, and texture, without aliasing or artifacts.



Figure 6a: 3D rendering of the modules of the ACR CT accreditation phantom (Gammex 464) and schematic of the low contrast section for CNR measurements.

TrueFidelity DL for Spectral imaging also improves the contrast-to-noise ratio (CNR) at the same dose. This is best demonstrated using the ACR CT accreditation phantom (Gammex 464) scanned with an adult abdominal GSI axial scan protocol (40 mm collimation, 0.6 s/rot, medium body filter) on the Revolution CT at 9.01 mGy. Following the ACR guidelines for CNR measurement, FBP, ASiR-V 50% (AR50), and DLIR for GSI low/medium/high (DL-L, DL-M, DL-H), images were reconstructed in 5 mm slice thickness over a 21 cm field of view at 70 keV. The CNR was calculated in the low contrast section depicted in Figure 6a from the 25 mm cylinders of small, energy-independent attenuation with 0.6%, 6 HU differences from background. ROI's of 100 mm² were chosen within the largest low contrast cylinder (ROI₁) as well as the background (ROI₂) as shown in Figure 6b and applied consistently to all reconstructed images. Then, the CNR was calculated as: $CNR = \frac{|\text{Mean}[ROI_1] - \text{Mean}[ROI_2]|}{\text{SD}[ROI_1]}$, where Mean and SD denote mean and standard deviation of the pixel CT Numbers inside the corresponding ROI. The calculated values in Table 1 clearly demonstrate the higher CNR achieved by TrueFidelity DL for Spectral imaging compared to both FBP and ASiR-V at all settings that significantly exceeds the ACR acceptance threshold of 1.0.

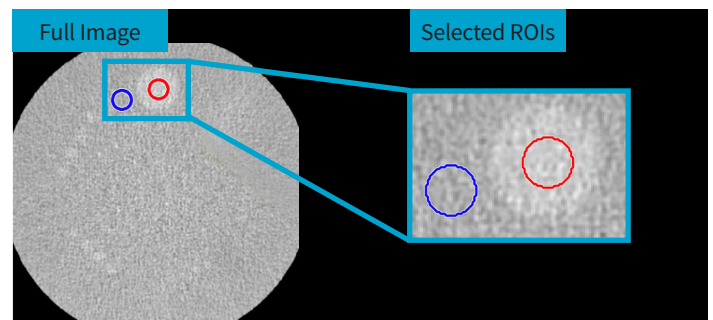


Figure 6b: Illustration of ROI placement for CNR assessment, ROI₁ in red and ROI₂ in blue.

Reconstruction Type	CNR
FBP	0.95
AR50	1.37
DL-L	1.5
DL-M	1.77
DL-H	2.21

Table 1: CNR measurements from GSI 70 keV images of the low contrast section of the ACR accreditation phantom scanned on the Revolution CT and reconstructed using FBP, AR50, AR100, DL-L, DL-M, and DL-H.

The noise in dual-energy images has unique characteristics after material decomposition, and it is important to ensure that denoising does not compromise valuable spectral information for diagnosis. In fact, TrueFidelity DL for Spectral imaging preserves material density quantification accuracy compared to ASiR-V iterative reconstruction when reconstructing data taken at the same dose. To establish robust performance across several clinically-relevant scenarios, MD accuracy was measured using a Gammex Multi-Energy CT phantom*** with inserts of different composition and density and images reconstructed with standard ASiR-V 50% (AR50) and TrueFidelity DL with Spectral imaging with the High setting (DL-H) compared with the known reference. The inserts include solid water, liquid water, and 5, 10, 15, and 20 mg/cm³ of iodine solution. Three different GSI acquisitions taken on the Revolution CT are included for completeness: Axial, Large Body SFOV, 40 mm aperture, at 23.59 mGy; Axial, Medium Body SFOV, 40 mm aperture, at 21.08 mGy; and Helical (0.992 pitch), Large Body SFOV, 80 mm aperture, at 19.16 mGy. MD accuracy was measured for each rod in each material image by computing the mean density of a circular ROI placed in the center of the respective insert as shown in Figure 7, averaged over 4 images for each data set. All images were reconstructed in 5 mm slice thickness in a 35 cm field of view.

The measured material density values shown in Table 2 are consistent between AR50 and DL-H for all material types, concentrations, and acquisitions, and match the known values for water and iodine within the accepted tolerance. Since all other basis pairs are formed of a recombination of the water/iodine basis pair selected for material decomposition, it is sufficient to assess quantitative accuracy on this native basis pair to establish performance over the full material space. Full characterization over other material basis pairs, including direct measurements from cortical bone (CB2-30%), can be found in the “Quantitative Evaluation of TrueFidelity DL (Deep Learning Image Reconstruction) for Spectral Imaging” Paper.²³

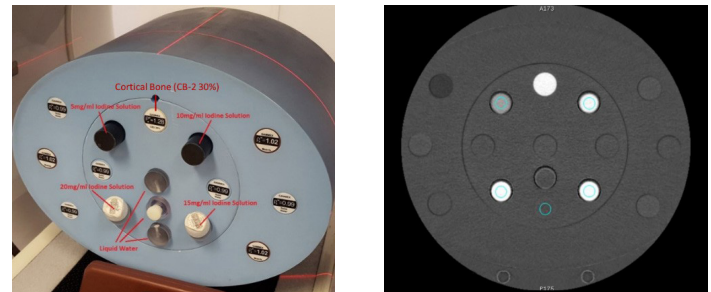


Figure 7: Gammex Multi-Energy CT phantom (left) used to assess MD quantitative accuracy, showing the water, iodine, and cortical bone inserts with their respective measurement ROIs in the iodine (water) image (right).

Mode	SFOV	CTDI (mGy)	Image Type	MD Quantitative Accuracy (mg/cm ³)			
				Material	AR50	DL-H	Ref. Goal
Axial 40 mm	Large Body	23.59	Water (Iodine)	Water	996.65	996.77	999 ± 11
				lo 5 mg	997.26	997.13	999 ± 15
			Iodine (Water)	Water	0.15	0.14	0 ± 0.3
				lo 5 mg	4.93	4.94	5 ± 1
				lo 10 mg	10.13	10.12	10 ± 1
				lo 15 mg	14.9	14.92	15 ± 1.5
Axial 40 mm	Medium Body	21.08	Water (Iodine)	Water	994.92	994.82	999 ± 11
				lo 5 mg	992.79	992.75	999 ± 15
			Iodine (Water)	Water	0.21	0.23	0 ± 0.3
				lo 5 mg	5.19	5.18	5 ± 1
				lo 10 mg	10.43	10.41	10 ± 1
				lo 15 mg	15.39	15.42	15 ± 1.5
Helical 80 mm/pitch 0.992	Large Body	19.16	Water (Iodine)	Water	993.38	993.48	999 ± 11
				lo 5 mg	989.05	989	999 ± 15
			Iodine (Water)	Water	0.22	0.23	0 ± 0.3
				lo 5 mg	5.41	5.4	5 ± 1
				lo 10 mg	10.44	10.44	10 ± 1
				lo 15 mg	15.14	15.15	15 ± 1.5
			lo 20 mg	20.61	20.6	20 ± 2	

Table 2: Revolution CT MD accuracy measurements for the Gammex Multi-Energy CT phantom (Gammex Inc., Middleton, WI, USA) shown for ASiR-V 50% (AR50) and TrueFidelity DL for Spectral imaging at the High setting (DL-H).

*** Gammex Inc., Middleton, WI, USA.

Just as important for spectral imaging, TrueFidelity DL for Spectral imaging preserves iodine detectability performance for concentrations as low as 0.5 mg/mL at a dose as low as 8 mGy. This was evaluated on the head portion of the Gammex Multi-Energy CT Phantom with a deionized water insert and six inserts of different concentrations of iodine – 16, 8, 4, 2, 1, and 0.5 mg/cc as shown in Figure 8. Results in Table 3 demonstrate comparable iodine quantification over the range of iodine concentrations from 0.5 – 16 mg/ml between AR50 and DL-H from 40 mm helical pitch 0.984:1 0.5 s/rot Medium Body SFOV GSI acquisitions at 8.16 mGy on Revolution Apex, reconstructed with 2.5 mm slice thickness. An independent two-sample t-test on the same data set comparing ROIs in the iodine contrast and deionized water was repeated for every concentration of iodine and concluded that the lowest detectable concentration of iodine was 0.5 mg/ml with a p-value of less than 0.001.

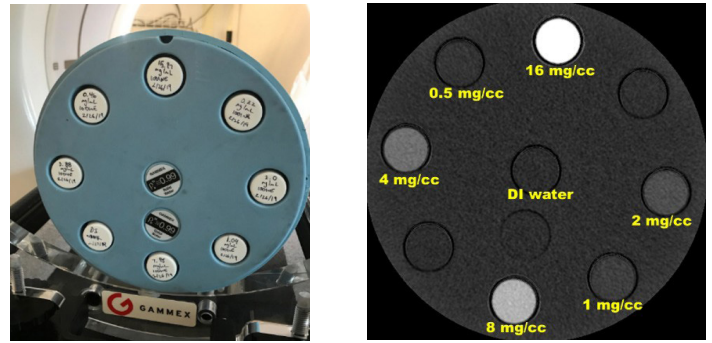


Figure 8: 20 cm Gammex phantom (left) with displayed inserts for detectability testing (right).

		16 mg/ml	8 mg/ml	4 mg/ml	2 mg/ml	1 mg/ml	0.5 mg/ml	DI water mg/ml
AR50	Mean	16.24	7.97	3.93	2.00	1.02	0.47	0.04
	Std. Dev. of Mean	0.08	0.04	0.03	0.04	0.02	0.01	0.01
DL-H	Mean	16.23	7.97	3.92	2.00	1.02	0.47	0.04
	Std. Dev. of Mean	0.08	0.04	0.03	0.04	0.02	0.01	0.01

Table 3: Iodine quantification measurements from the Revolution Apex for different concentrations of iodine from 16 mg/mL down to 0.5 mg/mL. Mean and standard deviation measurements reported from the same ROI on 13 separate slices are comparable for ASiR-V 50% and TrueFidelity DL for Spectral imaging. Standard deviation from the mean is representative of how reproducible the measurements are from scan to scan.

This combined set of quantitative results establishes that TrueFidelity DL for Spectral imaging is successful at managing noise reduction and CNR improvements in GSI studies without compromising spectral performance. TrueFidelity DL reconstruction also extends its benefits to image texture and natural appearance for an easier diagnostic read from single-energy to dual-energy modes. In an extensive clinical reader study, the noise texture of TrueFidelity DL for Spectral imaging was rated as improved over standard reconstruction techniques. This was demonstrated in a clinical evaluation consisting of 40 cases and 5 physicians, where each case was reconstructed with both TrueFidelity DL for Spectral imaging and ASiR-V and evaluated by 3 of the physicians. Cases included chest soft tissue and lung windows, abdomen soft tissue (incl. lesions and stones), pancreas, high BMI, metal implants, pediatric scans (spinal fixation), and head & neck CTA, all taken on the Revolution family of systems. This sample data was representative of a wide range of anatomical coverage and patient indications, and serves to demonstrate the performance of TrueFidelity DL for Spectral imaging for general patient imaging. A Likert-score image quality analysis showed that TrueFidelity DL for Spectral imaging is significantly better than ASiR-V for overall image quality as depicted in Figure 9 and the noise texture of TrueFidelity DL for Spectral imaging was rated higher than ASiR-V's in 88% of the reads, with details shown in Table 4.

TrueFidelity for GSI vs. ASiR-V	40 keV (N = 87)	70 keV (N = 120)	Water (Iodine) (N = 12)	Iodine (Water) (N = 99)	VUE (N = 87)	All (N = 405)
Better than	92%	86%	83%	88%	86%	88%
Same as	8%	14%	17%	12%	14%	12%
Worse than	0%	0%	0%	0%	0%	0%

Table 4: Assessment of noise texture in TrueFidelity DL for Spectral imaging vs. ASiR-V in a clinical reader study with 405 individual comparisons.

Average Image Quality Score

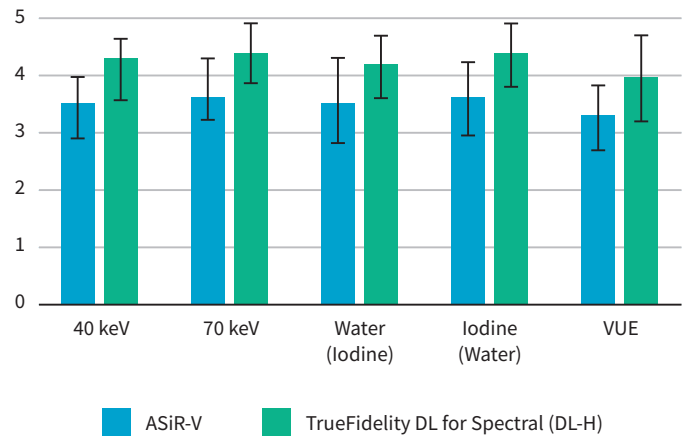


Figure 9: Overall image quality performance of TrueFidelity DL for Spectral imaging vs. ASiR-V 50% assessed with Likert scores in a reader study including 40 cases and 5 experienced radiologists. Likert scores are 5 – significantly better; 4 – better; 3 – similar; 2 – worse; 1 – significantly worse.

This feedback is consistent with a detailed analysis of the normalized Noise Power Spectrum (nNPS) performance with TrueFidelity DL for Spectral imaging across different image types and dose levels as depicted in Figures 10a and 10b. nNPS plots represent the frequency distribution of image noise as indicative of perceived texture in the eyes of a human observer. Generally, a shift of the peak of the nNPS curve to lower frequencies is indicative of more patchy/blotchy texture often described as artificial and unnatural looking images that often plague iterative reconstruction.^{24,25}

Figure 10a establishes that TrueFidelity DL for Spectral imaging produces images much closer to standard FBP images than iterative reconstruction across the full range of materials and keV images at the same dose. Figure 10b yields the same result when comparing 70 keV images across a range of clinically relevant dose levels. In all cases, nNPS plots were computed from 20 cm centered water phantom images. This explains how TrueFidelity DL for Spectral imaging scores well for natural appearance as its noise texture approaches that of higher-dose FBP images while significantly reducing image noise.

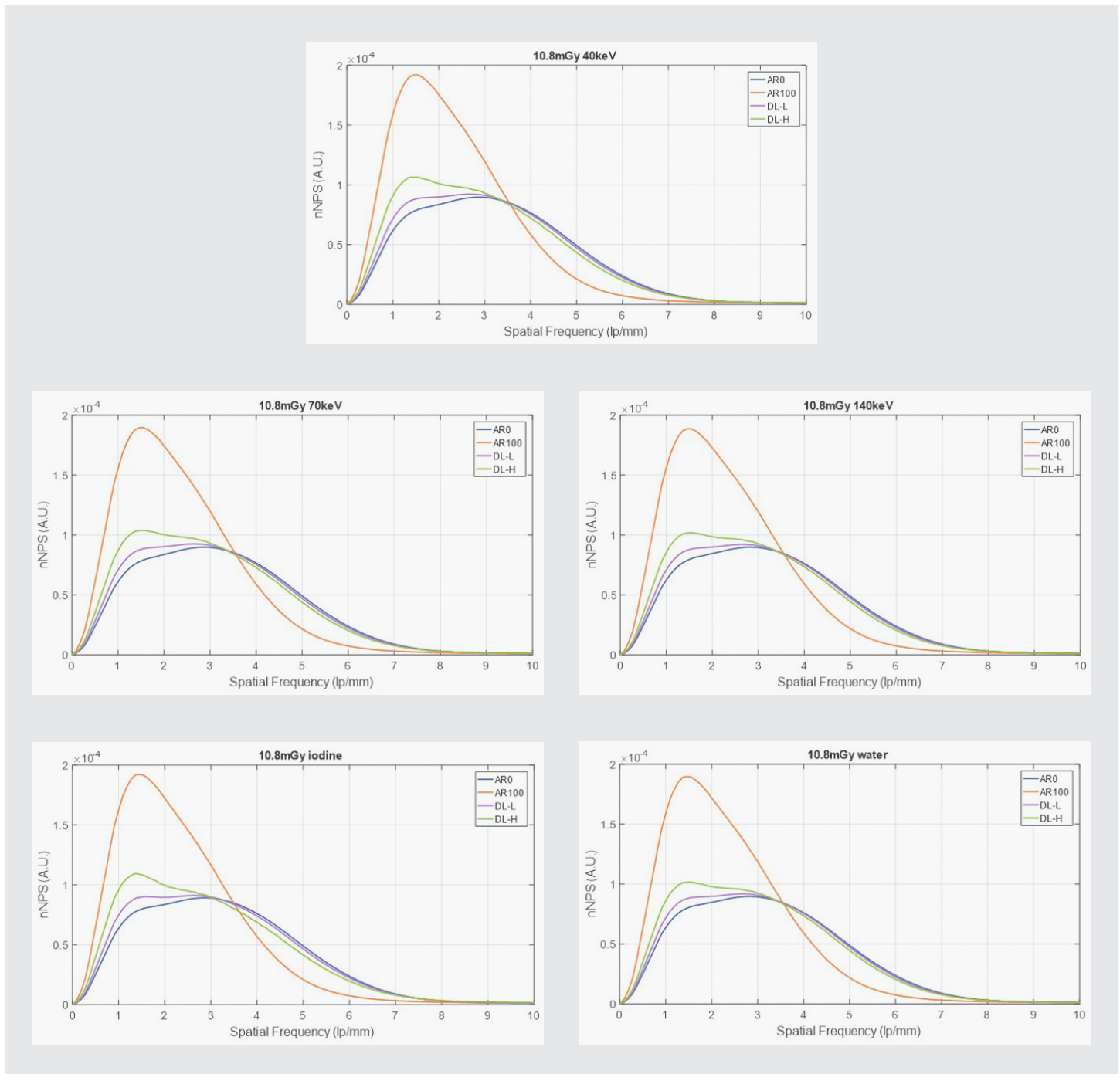


Figure 10a: Normalized Noise Power Spectrum performance across GSI image types at fixed dose (10.8 mGy) comparing TrueFidelity DL for Spectral imaging at the Low and High settings (DL-L and DL-H), ASIR-V 100% (AR100), and FBP (AR0). Graphs show 40, 70, 140 keV (top), as well as iodine (water) and water (iodine) basis materials (bottom). Measured from 20 cm centered | Water phantom.

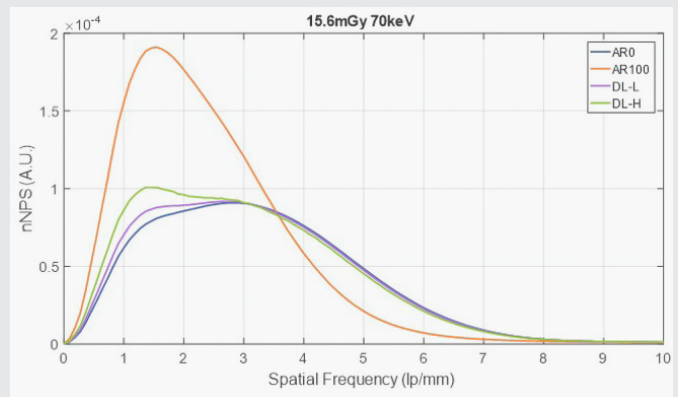
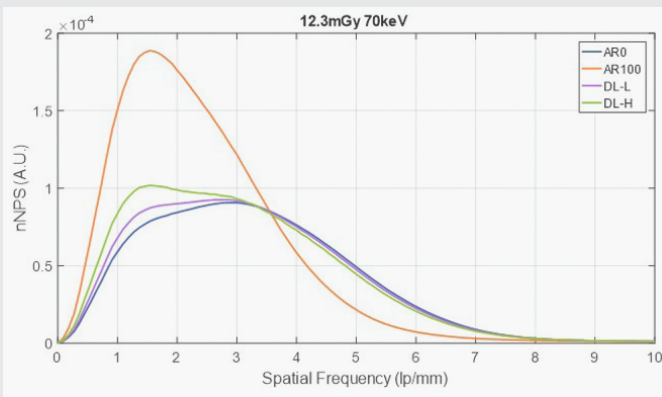
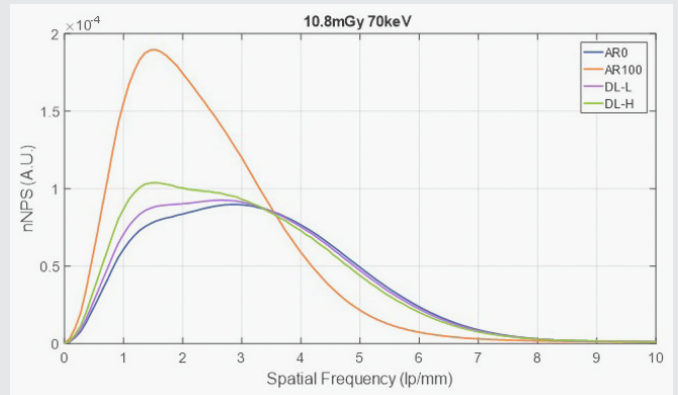
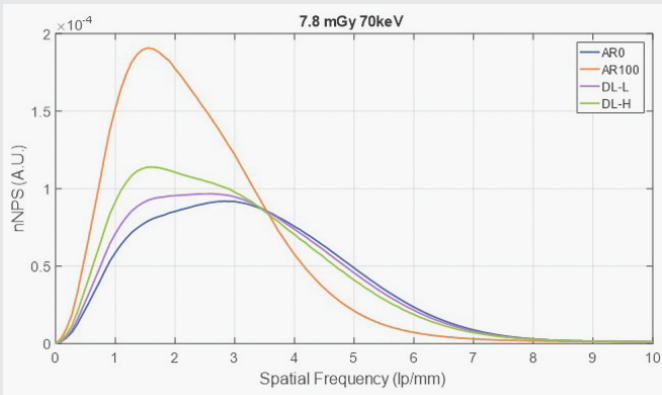
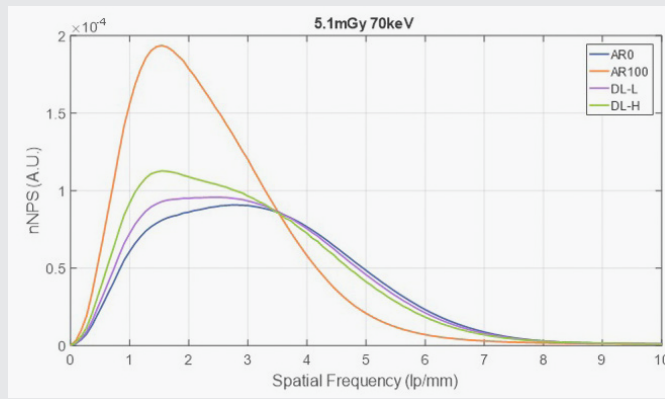


Figure 10b: Normalized Noise Power Spectrum performance across dose levels from 15.6 down to 5.1 mGy comparing TrueFidelity DL for Spectral imaging at the Low and High settings (DL-L and DL-H), ASIR-V 100% (AR100), and FBP (AR0). Measured from 20 cm centered | Water phantom.

Clinical Examples

Case 1: Uncompromised GSI images for all patient sizes

TrueFidelity DL for Spectral imaging is designed to reduce image noise, enhance CNR and produce natural noise texture for all GSI image types regardless of patient size. Bariatric spectral CT imaging can be freed of the traditional challenges that accompany high-BMI studies.

Figure 11 illustrates a typical example of an 85-year-old bariatric patient (BMI 48) scanned on the Revolution CT, three months after the resection of caecum adenocarcinoma. Monochromatic 50 keV images were reconstructed with both TrueFidelity DL and FBP with 1.25 mm slice thickness, showing significantly improved image quality on TrueFidelity DL, even with a low radiation dose of 16.15 mGy. GSI FOV of 50 cm helps cover all anatomy. Such a case would have previously demanded a higher energy level (70 keV) and thicker slices up to 5 mm for diagnostic use. All details were preserved, with low noise and excellent texture for a bariatric patient, delivering results equivalent to those expected from one with a lower BMI. Here, TrueFidelity DL for Spectral imaging helped retain anatomic details without excessive noise or degraded texture for a confident read.



“TrueFidelity DL for Spectral imaging allows us to scan high BMI patients with low dose, and reach confident diagnosis benefiting from GSI.”

Professor Alain Luciani

Centre Hospitalier Université Henri Mondor, France

Scan type	GSI Helical
Detector collimation, mm	80
Acquisition time, sec	6.4
Slice, mm	1.25
Reconstruction algorithm	TrueFidelity DL (DLIR-H)
Kernel	Standard
CTDIvol, mGy	16.15

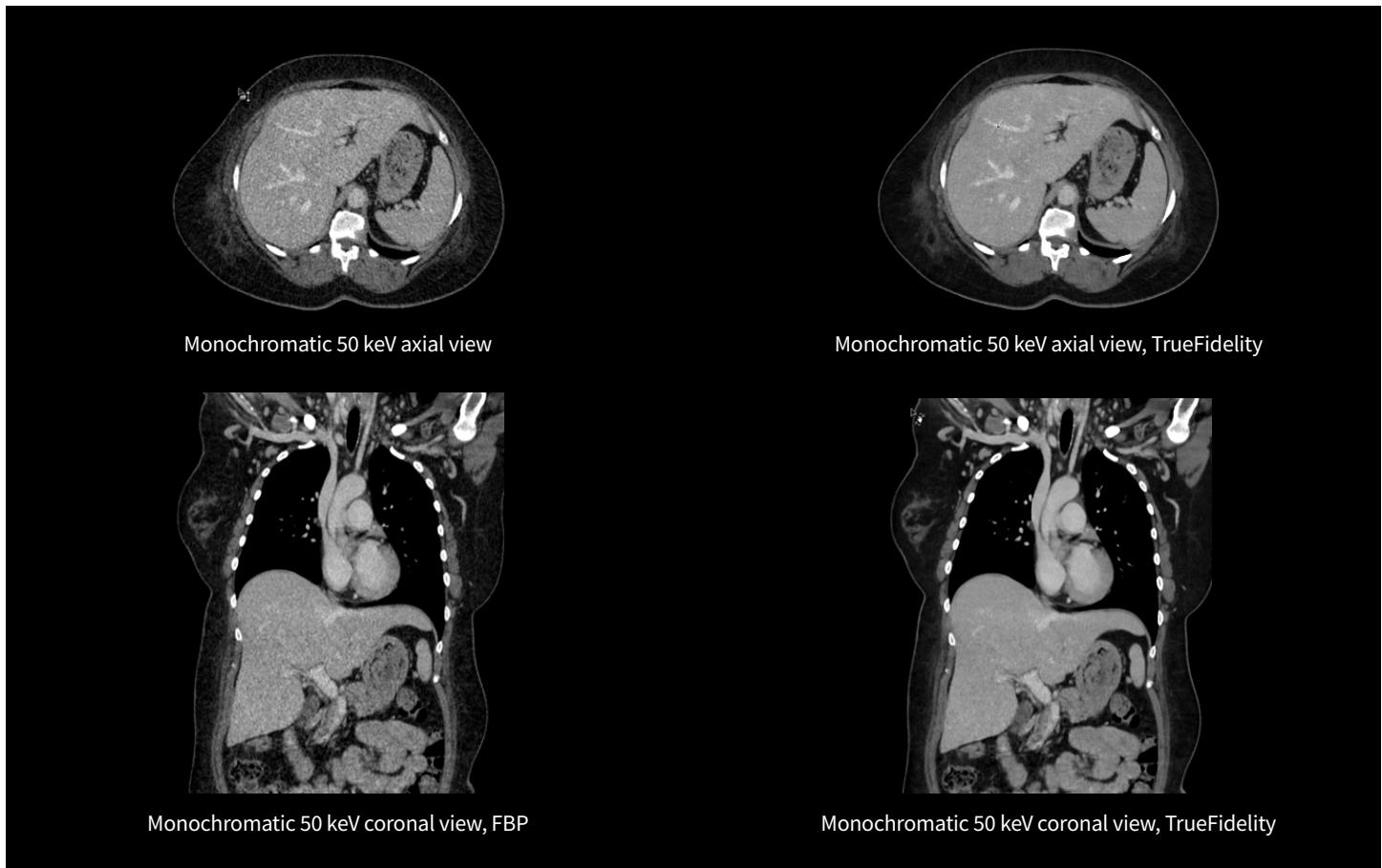


Figure 11: GSI images of a bariatric patient with BMI of 48.

Case 2: Enhanced lesion depiction and detection in oncology CT and PE

GSI is a proven diagnostic tool for both oncology and pulmonary embolism. In oncology CT, the use of low-energy monochromatic and iodine-specific images can improve lesion depiction and detection by improving the contrast between the lesion and normally enhancing parenchyma.²⁶ In pulmonary angiography, material-specific iodine images can help to identify pulmonary embolism associated perfusion defects, especially in patients with underlying perfusion abnormalities.²⁷ TrueFidelity DL for Spectral imaging is designed to enhance the performance of GSI by improving the image quality for both monochromatic and iodine-specific images.

Figure 12 illustrates a challenging case of a 66-year-old man with right lung adenocarcinoma surgery who was scanned on the Revolution CT with pulmonary angiography protocol due to acute onset of dyspnea. Monochromatic and iodine images were reconstructed with TrueFidelity DL with 0.625 mm slice thickness with 5 mGy. The iodine map showing hypo-perfusion of the left lung segments can help identify pulmonary embolus on monochromatic 50 keV images. Both 50 keV and iodine images accurately depict right hilar residual tumor lesions.

“TrueFidelity DL for Spectral imaging enhances the image quality for both monochromatic and iodine-specific images and can enhance the GSI benefits in lesion depiction and detection.”

Professor Jean-Nicolas Dacher

Centre Hospitalier Universitaire de Rouen, France

Scan type	GSI Helical
Detector collimation, mm	80
Rotation time, sec	0.5
Helical pitch	1.375
Slice, mm	0.625
Reconstruction algorithm	TrueFidelity DL (DLIR-H)
Kernel	Standard
CTDIvol	5

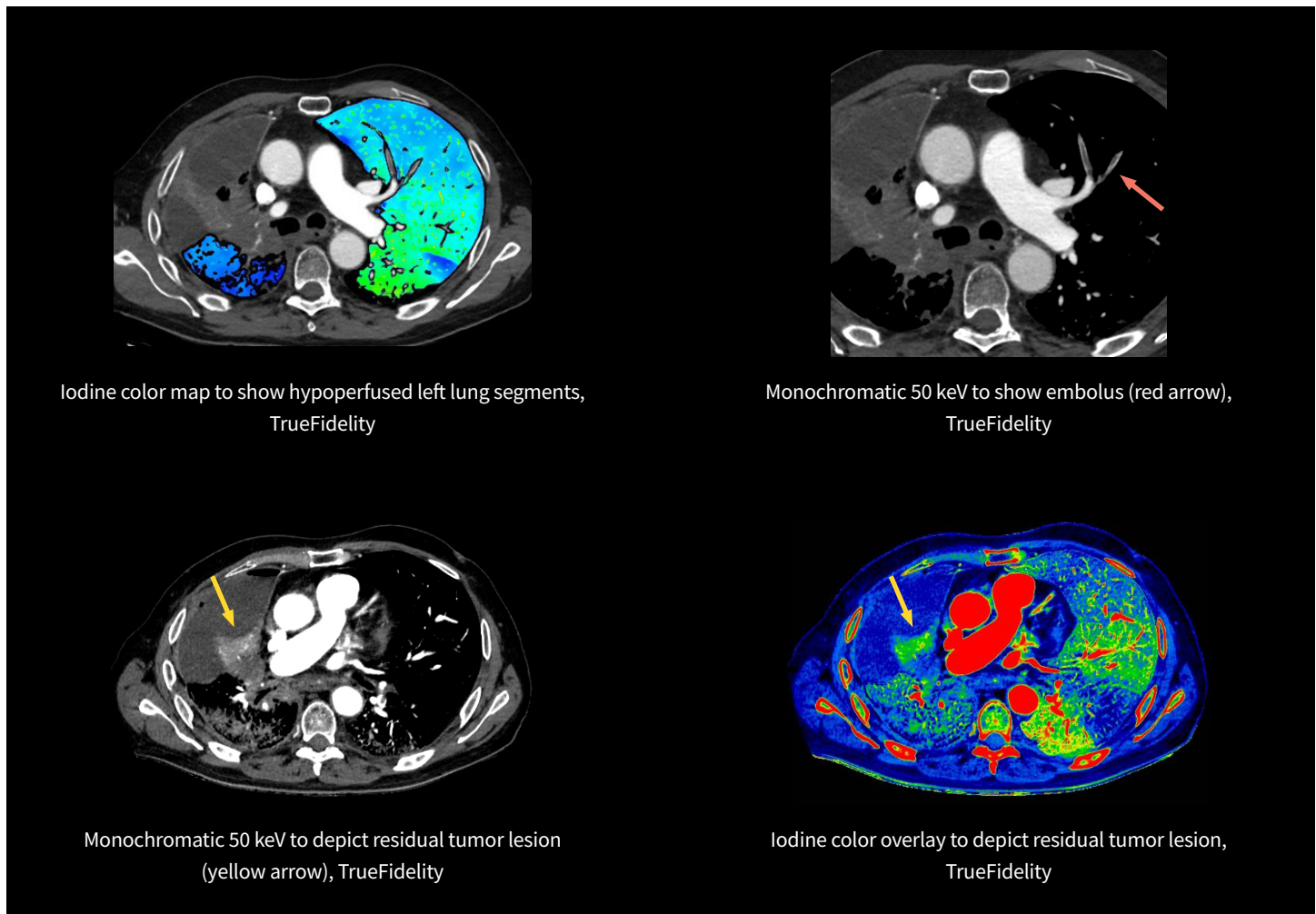


Figure 12: GSI images of lesion depiction and detection for a patient with tumor and PE.

Case 3: Identifying bowel wall ischemia and hemorrhage

Figure 13 illustrates an ER case of a 68-year-old man with acute abdominal pain. A 3-phase abdomen CT was ordered by the ED physician to rule out mesenteric ischemia.

A biphasic GSI protocol (arterial and portovenous phases) was conducted on the Revolution Apex, and VUE series were used to replace the non-contrast phase by saving radiation dose and scan time. TrueFidelity DL for Spectral imaging allowed routine use of monochromatic 40 keV and iodine images that confirmed the absence of contrast in the small intestine and colon bowel walls. The VUE images showed a persistence in high-density in some bowel walls (yellow arrows), confirming bowel wall hemorrhage as a complication of bowel wall ischemia.



“TrueFidelity DL for Spectral imaging used in the ED clinical routine can reconstruct relatively lower keV settings with a high CNR without a radiation dose penalty. It also provides images with very low noise material decomposition which are helpful to create easily interpretable color overlay images.”

Professor Koenraad Nieboer
University Hospital Brussels, Belgium

Scan type	GSI Helical
Detector collimation, mm	80
Rotation time, sec	0.5
Helical pitch	0.992
Slice, mm	0.625
Reconstruction algorithm	TrueFidelity DL (DLIR-H)
Kernel	Standard
CTDIvol	6.3

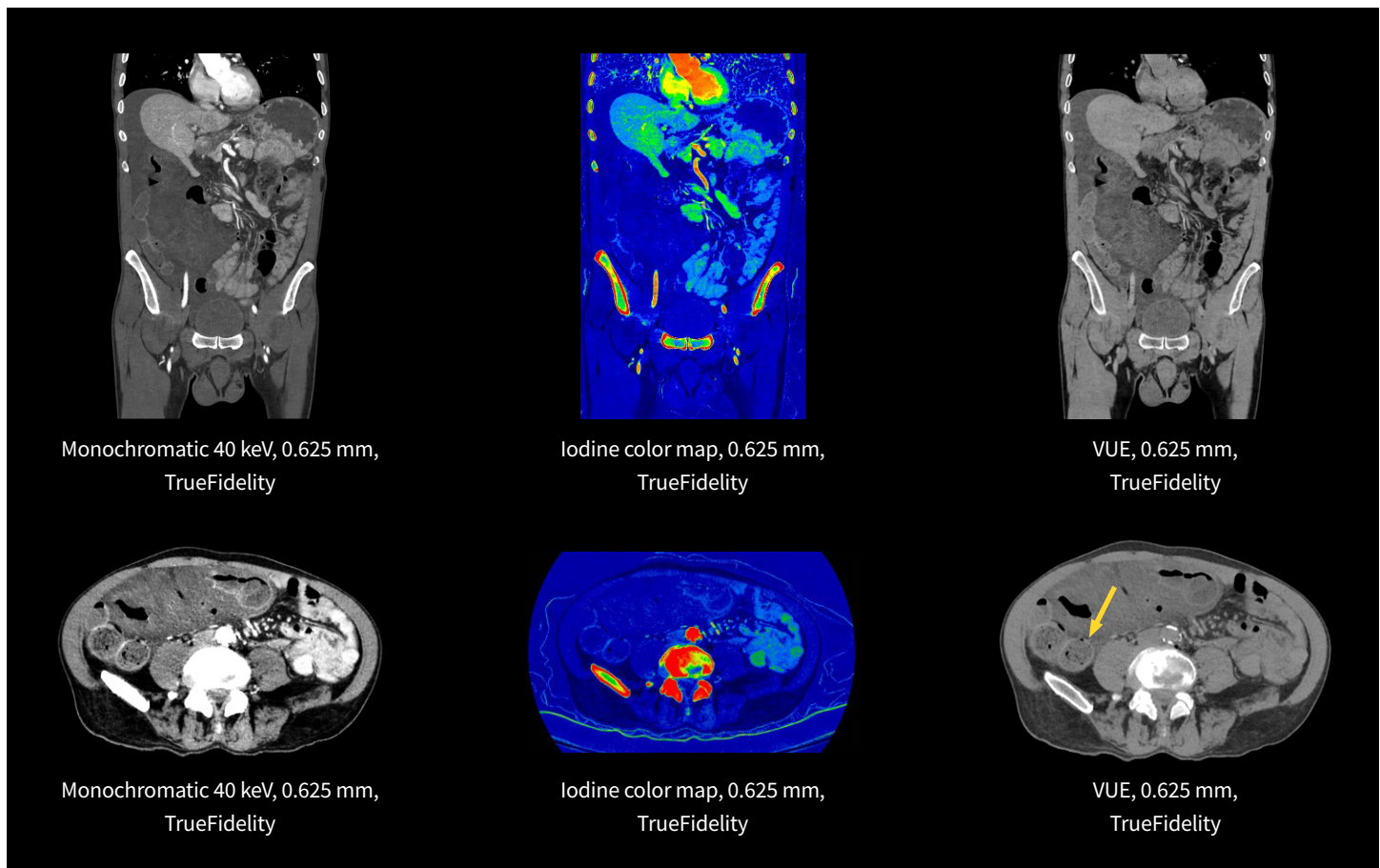


Figure 13: GSI images for identifying bowel wall ischemia and hemorrhage.

Case 4: Diagnosing a pseudoaneurysm in a patient with chronic pancreatitis

Figure 14 illustrates a case of a 67-year-old female presented to the ED with acute abdominal pain. The patient has a history of chronic pancreatitis that recently developed to be acute.

A biphasic GSI protocol (arterial and portal venous phases) was conducted on the Revolution Apex. High-quality TrueFidelity DL arterial 60 keV and iodine images identified a modular enhancing lesion in the head of the pancreas (yellow arrow) which increases in portal venous 68 keV and iodine (orange arrow). VUE, as the replacement of a true non-contrast phase, confirmed a calcification foci which is clearly visible on the arterial and portovenous phases. The suggested diagnosis is a pseudoaneurysm as a complication of recent acute pancreatitis in a patient with chronic pancreatitis.

TrueFidelity DL increases the clinical utility of traditionally noisier images such as low keV and 0.625mm images, as demonstrated here as well as in peer reviewed literature.²⁸

“TrueFidelity DL for Spectral imaging helps us to confirm the diagnosis of a pseudoaneurysm on the monochromatic and iodine images in the arterial and portovenous phase. The VUE helps us to identify the calcification from an arterial vessel. By using the VUE we are able to reduce the radiation dose for patients by not acquiring a non-contrast scan.”

Professor Koenraad Nieboer
University Hospital Brussels, Belgium

Scan type	GSI Helical
Detector collimation, mm	80
Rotation time, sec	0.5
Helical pitch	1.531
Slice, mm	0.625
Reconstruction algorithm	TrueFidelity DL (DLIR-H)
Kernel	Standard

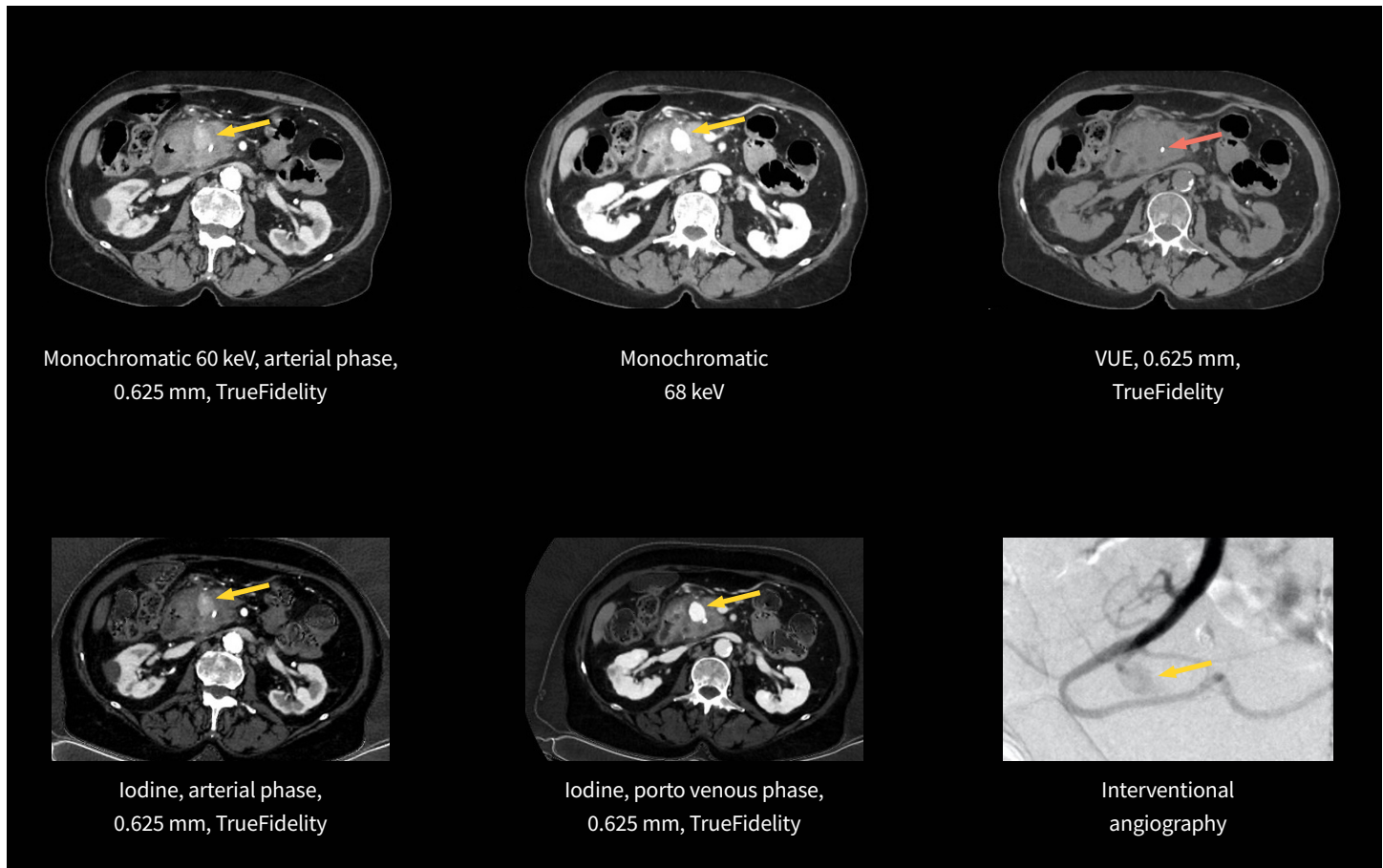


Figure 14: GSI images for diagnosing pseudoaneurysm.

Case 5: Detecting bone fracture and bone marrow edema

Figure 15 illustrates a case of a 66-year-old female with persisting wrist pain. The patient fell on her outstretched hand 12 days ago. Her family physician ordered an MRI scan of the wrist after a negative X-ray. Due to the long MRI waiting list, GSI was suggested to rule out a scaphoidal fracture with bone marrow edema.

TrueFidelity DL for Spectral imaging can generate high quality water and Hydroxyapatite (HAP) material images. Water (HAP) images demonstrate an increased water content in the scaphoid bone (orange arrow), and suggest the presence of bone marrow edema. Monochromatic 70 keV with bone kernel shows an underlying scaphoidal fracture (yellow arrow).

“TrueFidelity DL for Spectral imaging helps us to identify bone marrow edema and underlying bone fracture. It may benefit the patients who have difficulties getting access to MRI.”

Professor Koenraad Nieboer
University Hospital Brussels, Belgium

Scan type	GSI Helical
Detector collimation, mm	40
Rotation time, sec	1
Helical pitch	0.992
Slice, mm	0.625
Reconstruction algorithm	TrueFidelity DL (DLIR-H) ASiR-V strength
Kernel	Standard, bone

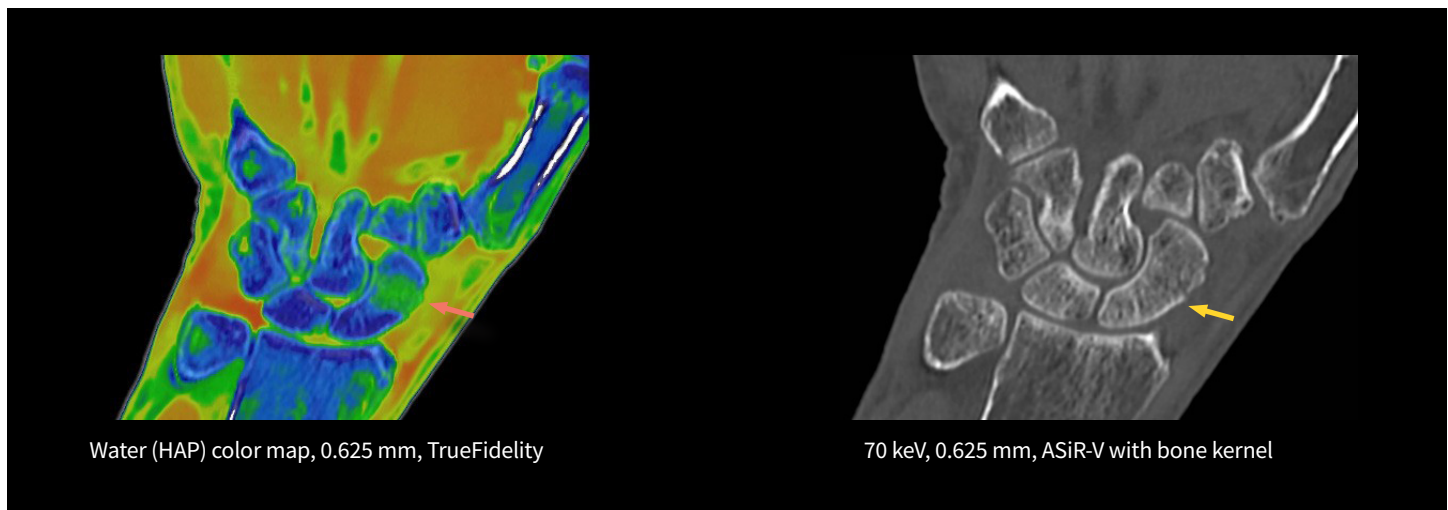


Figure 15: GSI images for bone fracture and bone marrow edema detection.

Conclusion

At the heart of GE’s dual-energy GSI technology, true view-to-view fast kV switching enables excellent temporal registration and spatial resolution without needing to discard kV transitions or apply DL-based view recovery techniques. No compromise is made in the view sampling rate for data collection and image generation.

TrueFidelity DL for Spectral imaging now brings the potential to substantially reduce the image noise in all spectral image types, from virtual monochromatic images to material image pairs and virtual non-contrast images, with and without metal artifact reduction. Specifically, reducing the image noise increase inherent with low keV images resolves one of the traditional technical challenges in adopting more dual-energy protocols across the full patient population.

Unlike other denoising methods, TrueFidelity DL is explicitly designed to preserve image texture, as demonstrated by quantitative performance metrics. Moreover, all the spectral image types are inherently supported without any compromise to the quantitative accuracy that GSI is known for in the industry.

With the available computational power of the Xstream reconstruction server, TrueFidelity DL for Spectral imaging can be applied routinely to all GSI applications without impact to the overall workflow, even in acute care settings. This technology will have a significant role in expanding the benefits of spectral imaging across all anatomies and care areas.

References

1. Scott Slavic, Priti Madhav, Mark Profio, Dominic Crotty, Elizabeth Nett, Jiang Hsieh, Eugene Liu, (October 2017). "GSI Xstream on Revolution CT – Volume, Spectral, Simplified", Slavic et al, GE Technology White Paper. <https://www.gehealthcare.com/-/media/069734962cbf45c1a5a01d1cdde9a4cd.pdf>.
2. Agrawal MD, Pinho DF, Kulkarni NM, Hahn PF, Guimaraes AR, Sahani DV. Oncologic applications of dual-energy CT in the abdomen. *Radiographics*. 2014 May-Jun;34(3):589-612. doi: 10.1148/rg.343135041. PMID: 24819783.
3. Shuman WP, Green DE, Busey JM, Mitsumori LM, Choi E, Koprowicz KM, Kanal KM. Dual-energy liver CT: effect of monochromatic imaging on lesion detection, conspicuity, and contrast-to-noise ratio of hypervascular lesions on late arterial phase. *AJR Am J Roentgenol*. 2014 Sep;203(3):601-6. doi: 10.2214/AJR.13.11337. PMID: 25148163. Kulkarni NM, Eisner BH, Pinho DF, Joshi MC, Kambadakone AR, Sahani DV. Determination of renal stone composition in phantom and patients using single-source dual-energy computed tomography. *J Comput Assist Tomogr*. 2013 Jan-Feb;37(1):37-45. doi: 10.1097/RCT.0b013e3182720f66. PMID: 23321831.
4. Pomerantz SR, Kamalian S, Zhang D, Gupta R, Rapalino O, Sahani DV, Lev MH. Virtual monochromatic reconstruction of dual-energy unenhanced head CT at 65-75 keV maximizes image quality compared with conventional polychromatic CT. *Radiology*. 2013 Jan;266(1):318-25. doi: 10.1148/radiol.12111604. Epub 2012 Oct 16. PMID: 23074259.
5. Yuan R, Shuman WP, Earls JP, Hague CJ, Mumtaz HA, Scott-Moncrieff A, Ellis JD, Mayo JR, Leipsic JA. Reduced iodine load at CT pulmonary angiography with dual-energy monochromatic imaging: comparison with standard CT pulmonary angiography—a prospective randomized trial. *Radiology*. 2012 Jan;262(1):290-7. doi: 10.1148/radiol.11110648. Epub 2011 Nov 14. PMID: 22084206.
6. Han SC, Chung YE, Lee YH, Park KK, Kim MJ, Kim KW. Metal artifact reduction software used with abdominopelvic dual-energy CT of patients with metal hip prostheses: assessment of image quality and clinical feasibility. *AJR Am J Roentgenol*. 2014 Oct;203(4):788-95. doi: 10.2214/AJR.13.10980. PMID: 25247944.
7. Son W, Park C, Jeong HS, Song YS, Lee IS. Bone marrow edema in non-traumatic hip: high accuracy of dual-energy CT with water-hydroxyapatite decomposition imaging. *Eur Radiol*. 2020 Apr;30(4):2191-2198. doi: 10.1007/s00330-019-06519-8. Epub 2019 Dec 10. PMID: 31822976.
8. Svensson E, Aurell Y, Jacobsson LTH, Landgren A, Sigurdardottir V, Dehlin M. Dual energy CT findings in gout with rapid kilovoltage-switching source with gemstone scintillator detector. *BMC Rheumatol*. 2020 Jan 17;4:7. doi: 10.1186/s41927-019-0104-5. PMID: 31989100; PMCID: PMC6966802.
9. "Revolution Apex with Quantix 160 – When Power Meets Coverage", Thibault et al, GE Technology White Paper, April 2020. https://www.gehealthcare.com/-/jssmedia/global/products/images/revolution-apex-platform/quantix_whitepaper_jb78157xx.pdf?rev=-1.
10. Jacobsen MC, Schellingerhout D, Wood CA, Tamm EP, Godoy MC, Sun J, Cody DD. Intermanufacturer Comparison of Dual-Energy CT Iodine Quantification and Monochromatic Attenuation: A Phantom Study. *Radiology*. 2018 Apr;287(1):224-234. doi: 10.1148/radiol.2017170896. Epub 2017 Nov 29. PMID: 29185902.
11. Muenzel D, Lo GC, Yu HS, Parakh A, Patino M, Kambadakone A, Rummeny EJ, Sahani DV. Material density iodine images in dual-energy CT: Detection and characterization of hypervascular liver lesions compared to magnetic resonance imaging. *Eur J Radiol*. 2017 Oct;95:300-306. doi: 10.1016/j.ejrad.2017.08.035. Epub 2017 Aug 31. PMID: 28987684.
12. Noda Y, Tochigi T, Parakh A, Joseph E, Hahn PF, Kambadakone A. Low keV portal venous phase as a surrogate for pancreatic phase in a pancreatic protocol dual-energy CT: feasibility, image quality, and lesion conspicuity. *Eur Radiol*. 2021 Sep;31(9):6898-6908. doi: 10.1007/s00330-021-07744-w. Epub 2021 Mar 20. PMID: 33744992.
13. A. Annoni, A. Formenti, D. Andreini, E. Nobili, M. Petulla, G. Ballerini, G. Pontone, M. Pepi. Dual Energy Gemstone Spectral Imaging (GSI) lung perfusion MDCT in acute pulmonary embolism: blood volume assessment and correlation with clinical symptoms, *European Heart Journal*, Volume 34, Issue suppl_1, 1 August 2013, P1146, <https://doi.org/10.1093/eurheartj/eh308.P1146>.
14. Jawad S, Ulriksen PS, Kalhauge A, Hansen KL. Acute Pulmonary Embolism Severity Assessment Evaluated with Dual Energy CT Perfusion Compared to Conventional CT Angiographic Measurements. *Diagnostics (Basel)*. 2021 Mar 11;11(3):495. doi: 10.3390/diagnostics11030495. PMID: 33799729; PMCID: PMC8000326.
15. Lacroix M, Mulé S, Herin E, Pigneur F, Richard P, Zegai B, Baranes L, Djabbari M, Brunetti F, deAngelis N, Laurent A, Tacher V, Kobeiter H, Luciani A. Virtual unenhanced imaging of the liver derived from 160-mm rapid-switching dual-energy CT (rsDECT): Comparison of the accuracy of attenuation values and solid liver lesion conspicuity with native unenhanced images. *Eur J Radiol*. 2020 Dec;133:109387. doi: 10.1016/j.ejrad.2020.109387. Epub 2020 Nov 2. PMID: 33166833.
16. Arndt C, Güttler F, Heinrich A, Bürckenmeyer F, Diamantis I, Teichgräber U. Deep Learning CT Image Reconstruction in Clinical Practice. *Rofo*. 2021 Mar;193(3):252-261. English. doi: 10.1055/a-1248-2556. Epub 2020 Dec 10. PMID: 33302311.
17. Benz DC, Ersözlü S, Mojon FLA, Messerli M, Mitulla AK, Ciancone D, Kenkel D, Schaab JA, Gebhard C, Pazhenkottil AP, Kaufmann PA, Buechel RR. Radiation dose reduction with deep-learning image reconstruction for coronary computed tomography angiography. *Eur Radiol*. 2022 Apr;32(4):2620-2628. doi: 10.1007/s00330-021-08367-x. Epub 2021 Nov 18. PMID: 34792635.
18. Kim I, Kang H, Yoon HJ, Chung BM, Shin NY. Deep learning-based image reconstruction for brain CT: improved image quality compared with adaptive statistical iterative reconstruction- Veo (ASIR-V). *Neuroradiology*. 2021 Jun;63(6):905-912. doi: 10.1007/s00234-020-02574-x. Epub 2020 Oct 10. PMID: 33037503.
19. Noda Y, Kawai N, Nagata S, Nakamura F, Mori T, Miyoshi T, Suzuki R, Kitahara F, Kato H, Hyodo F, Matsuo M. Deep learning image reconstruction algorithm for pancreatic protocol dual-energy computed tomography: image quality and quantification of iodine concentration. *Eur Radiol*. 2022 Jan;32(1):384-394. doi: 10.1007/s00330-021-08121-3. Epub 2021 Jun 15. PMID: 34131785.
20. "A new era of image reconstruction: TrueFidelity Technical white paper on deep learning image reconstruction", Hsieh et al, GE Technical White Paper, July 2019. TrueFidelity white paper: <https://www.gehealthcare.com/-/jssmedia/files/truefidelity/truefidelity-white-paper-jb68676xx-doc2287426.pdf?rev=-1>.
21. Greffier, Joël & Hamard, Aymeric & Pereira, Fabricio & Barrau, Corinne & Pasquier, Hugo & Beregi, Jean-Paul & Frandon, Julien. (2020). Image quality and dose reduction opportunity of deep learning image reconstruction algorithm for CT: a phantom study. *European Radiology*. 30. 10.1007/s00330-020-06724-w.
22. Sun, Jihang & Li, Haoyan & Li, Jianying & Yu, Tong & Li, Michelle & Zhou, Zuofu & Peng, Yun. (2021). Improving the image quality of pediatric chest CT angiography with low radiation dose and contrast volume using deep learning image reconstruction. *Quantitative Imaging in Medicine and Surgery*. 11. 3051-3058. 10.21037/qims-20-1158.
23. "Quantitative Evaluation of TrueFidelity (Deep Learning Image Reconstruction) for Gemstone Spectral Imaging", AAPM Virtual Meeting. Nett B. et al, 07/12/20; 302475; PO-GeP-I-179 Topic: Multi-detector CT.
24. Sung P, Lee JM, Joo I, Lee S, Kim TH, Ganeshan B. Evaluation of the Impact of Iterative Reconstruction Algorithms on Computed Tomography Texture Features of the Liver Parenchyma Using the Filtration-Histogram Method. *Korean J Radiol*. 2019 Apr;20(4): 558-568. doi: 10.3348/kjr.2018.0368. PMID: 30887738; PMCID: PMC6424830.
25. Singh, Sarabjeet, Mannudeep K. Kalra, Matthew D. Gilman, Jiang Hsieh, Homer H. Pien, Subba R. Digumarthy, and Jo-Anne O. Shepard. "Adaptive statistical iterative reconstruction technique for radiation dose reduction in chest CT: a pilot study." *Radiology* 259, no. 2 (2011): 565-573.
26. Agrawal, M. D., Sahani, D. V. (2014). Oncologic Applications of Dual-Energy CT in the Abdomen. *RadioGraphics*, 34(3), 589–612.
27. Patino, M., Sahani, D. V. (2016). Material Separation Using Dual-Energy CT: Current and Emerging Applications. *RadioGraphics*, 36(4), 1087–1105.
28. Njølstad et. al. "Improved image quality in abdominal computed tomography reconstructed with a novel Deep Learning Image Reconstruction technique – initial clinical experience", *Acta Radiologica Open* 10(4) 2021].

